

INVERSE ESTIMATION OF BED ROUGHNESS COEFFICIENTS OF OPEN-CHANNEL  
BY USING ADJOINT MODEL IN SHALLOW-WATER FLOWS

By

Keisuke Yoshida

Architecture and Civil Engineering, Chiba Institute of Technology, Narashino, Chiba, Japan

and

Tadaharu Ishikawa

Graduate School of Science and Engineering, Tokyo Institute of Technology, Yokohama, Japan

SYNOPSIS

This work describes and explains the methodology of an inverse estimation of distributed bed roughness coefficients of open-channels with flood plains. The Lagrange multiplier method is employed for the parameter identification. A shallow-water model is utilized as the constraint condition, and a variational approach enables us to develop the adjoint model. The requisite gradient information to satisfy the optimal condition is efficiently obtained through the adjoint equations. The optimal coefficients are determined by the quasi-Newton method. The identical twin experiments were carried out by using synthetic data in order to verify the validity of the proposed method. The assimilated data consist of the water level and the depth-averaged velocity calculated by the forward model. It is clear that the coefficients can be accurately predicted and that these estimates are stable with respect to random noise in data, provided that sufficient data are available at more observation stations.

INTRODUCTION

The shallow-water model has been applied to various analyses of flood flows. In this model, the parameters such as the bed level, the bed surface condition and the horizontal eddy viscosity are required to perform numerical simulations, and it is clearly evident that these parameters have a significant influence on the simulated results in shallow-water flows. However, in practical works, the observation data during floods are not necessarily sufficiently available; direct measurements of roughness coefficients in large-scale flow domains are almost impossible during floods. In general, it is therefore difficult to estimate accurately each parameter by using the partially observed data. Consequently, in most cases the parameters are subjectively determined with the limited data through trial and errors based on the engineer's experience. However, such estimation tends to be time-consuming in large-scale and nonlinear flow analysis.

The optimal theory has been employed recently to identify the parameters and the initial conditions in the model of large-scale flows in meteorology and oceanography. It has been found that the technique based on this theory can

improve the identification process significantly. The optimal theory is capable of minimizing the discrepancy between the simulated data and the observed data, and this discrepancy is mathematically defined as a cost function or an objective function. The parameter identification then becomes the inverse problem for searching the optimal values of the parameters by minimizing the function. Regarding this problem, the constraint conditions are imposed on it, by considering the dependent variables including the parameters are governed by the relevant hydraulic model.

The governing equations of the shallow-water model usually include the advection terms. These terms implicitly cause nonlinear optimal problems in minimizing the function. When such problems occur, it is necessary to accurately estimate the sensitivity of the objective function with respect to the parameters. Ding and Wang (1) concisely reviewed the previous solutions of these problems and pointed out that there have been three typical approaches: the influence-coefficient method, the sensitivity-equation method and the adjoint-equation method. Among these methods, the adjoint-equation method has a special advantage in the problems with large number of control variables and comparatively few responses. That means the gradient of the function can be efficiently computed by the adjoint-equation method with support of certain descent algorithms.

The identification technique has been used to estimate the parameters in several hydraulic models of open-channel flows. Atanov *et al.* (2) used the adjoint-equation method to identify a distributed profile of Manning's roughness coefficient along a trapezoidal open channel. Sanders and Katopodes (3) developed a new method of control of gate operating at both upstream and downstream ends in a water delivering canal with a rectangular channel cross-section by means of the adjoint sensitivity method. Ramesh *et al.* (4) solved the inverse problem to identify the roughness coefficient in a channel network by using a sequential quadratic algorithm. Dulhoste *et al.* (5) applied the nonlinear theory to control the water distribution with a collocation method by using the 1-D fully nonlinear Saint-Venant equations. Sulzer *et al.* (6) estimated flood discharges in the 2-D cross-sectionally averaged flow model by using the finite element method, accompanied with the Levenberg- Marquardt minimization algorithm. Ding and Wang (1) developed the adjoint-equation method to identify the distributed Manning's roughness coefficient along a 1-D channel network.

As mentioned above, several papers have been written on the parameter estimation in hydraulic models. However, few studies have been carried out on the identification of roughness coefficients varying in a compound open-channel. In this study, the inverse estimation method based on the optimal theory and the shallow-water model is proposed to identify the distributed Manning's roughness coefficients in open-channels with flood plains. The adjoint-equation model (or backward model) is derived by the variational principle, which is applied to the shallow water model (or forward model). The distributed coefficients in the flood plain are identified with the synthetic data generated by the forward model. That means the feasibility of the proposed method can be verified by the identical twin experiments.

## GOVERINING EQUATIONS

The following assumptions are made in the hydraulic model employed here: 1) incompressible Newtonian fluid; 2) constant viscosity; 3) hydrostatic pressure distribution along the water depth; 4) negligible wind shear on the water surface. Based on these assumptions, 2-D shallow-water equations of open-channel flows are obtained by integrating the Reynolds-averaged continuity and Navier-Stokes equations from the channel bed to the water surface. In this study, these equations are described as the conservative form in a generalized (or boundary fitted) curvilinear coordinate system as follows (see e.g., Nagata *et al.* (7)):

$$f_h = \frac{\partial \hat{J}h}{\partial t} + \frac{\partial \hat{J}M}{\partial \xi} + \frac{\partial \hat{J}N}{\partial \eta} = 0 \quad (1)$$

$$\begin{aligned}
f_M = & \frac{\partial \hat{J}M}{\partial t} + \frac{\partial \hat{J}UM}{\partial \xi} + \frac{\partial \hat{J}VM}{\partial \eta} + gh \left( \frac{\xi_x^2 + \xi_y^2}{J} \frac{\partial H}{\partial \xi} + \frac{\xi_x \eta_x + \xi_y \eta_y}{J} \frac{\partial H}{\partial \eta} \right) \\
& - m\hat{J} \left( U \frac{\partial \xi_x}{\partial \xi} + V \frac{\partial \xi_x}{\partial \eta} \right) - n\hat{J} \left( U \frac{\partial \xi_y}{\partial \xi} + V \frac{\partial \xi_y}{\partial \eta} \right) + \frac{gn_*^2 M \hat{J} \sqrt{u^2 + v^2}}{h^{4/3}} \\
& - \frac{\xi_x^2}{J} \frac{\partial \tau_{xx} h}{\partial \xi} - \frac{\xi_x \eta_x}{J} \frac{\partial \tau_{xx} h}{\partial \eta} - \frac{\xi_y^2}{J} \frac{\partial \tau_{yy} h}{\partial \xi} - \frac{\xi_y \eta_y}{J} \frac{\partial \tau_{yy} h}{\partial \eta} \\
& - \frac{2\xi_x \xi_y}{J} \frac{\partial \tau_{xy} h}{\partial \xi} - \frac{\xi_x \eta_y + \xi_y \eta_x}{J} \frac{\partial \tau_{xy} h}{\partial \eta} = 0
\end{aligned} \tag{2a}$$

$$\begin{aligned}
f_N = & \frac{\partial \hat{J}N}{\partial t} + \frac{\partial \hat{J}UN}{\partial \xi} + \frac{\partial \hat{J}VN}{\partial \eta} + gh \left( \frac{\xi_x \eta_x + \xi_y \eta_y}{J} \frac{\partial H}{\partial \xi} + \frac{\eta_x^2 + \eta_y^2}{J} \frac{\partial H}{\partial \eta} \right) \\
& - m\hat{J} \left( U \frac{\partial \eta_x}{\partial \xi} + V \frac{\partial \eta_x}{\partial \eta} \right) - n\hat{J} \left( U \frac{\partial \eta_y}{\partial \xi} + V \frac{\partial \eta_y}{\partial \eta} \right) + \frac{gn_*^2 N \hat{J} \sqrt{u^2 + v^2}}{h^{4/3}} \\
& - \frac{\xi_x \eta_x}{J} \frac{\partial \tau_{xx} h}{\partial \xi} - \frac{\eta_x^2}{J} \frac{\partial \tau_{xx} h}{\partial \eta} - \frac{\xi_y \eta_y}{J} \frac{\partial \tau_{yy} h}{\partial \xi} - \frac{\eta_y^2}{J} \frac{\partial \tau_{yy} h}{\partial \eta} \\
& - \frac{\xi_x \eta_y + \xi_y \eta_x}{J} \frac{\partial \tau_{xy} h}{\partial \xi} - \frac{2\eta_x \eta_y}{J} \frac{\partial \tau_{xy} h}{\partial \eta} = 0
\end{aligned} \tag{2b}$$

$$f_m = m - x_\xi M - x_\eta N = 0; \quad f_n = n - y_\xi M + y_\eta N = 0 \tag{3}$$

$$f_{\tau_{xx}} = \tau_{xx} - 2\varepsilon \frac{\partial u}{\partial x} + \frac{2k}{3} = 0; \quad f_{\tau_{yy}} = \tau_{yy} - 2\varepsilon \frac{\partial v}{\partial y} + \frac{2k}{3} = 0; \quad f_{\tau_{xy}} = \tau_{xy} - \varepsilon \left( \frac{\partial u}{\partial y} + \frac{\partial v}{\partial x} \right) = 0 \tag{4}$$

where  $f_h, f_M$  and  $f_N$  denote differential operators for the mass balance and momentum conservations and  $f_m, f_n, f_{\tau_{xx}}, f_{\tau_{yy}}$  and  $f_{\tau_{xy}}$  are the functions to define the corresponding dependent variables, respectively,  $t$  = time;  $x$  and  $y$  = two-dimensional Cartesian coordinates;  $\xi$  and  $\eta$  = boundary fitted coordinates;  $h$  = local water depth;  $u$  and  $v$  =  $x$ - and  $y$ -components of velocity vectors;  $m$  and  $n$  = and components of discharge flux;  $g$  = gravity acceleration;  $\varepsilon$  = horizontal eddy viscosity;  $k$  = depth-averaged turbulent kinetic energy;  $H$  = water level;  $\tau_{xx}, \tau_{xy}$  and  $\tau_{yy}$  = Cartesian components of depth-averaged Reynolds stress tensors;  $\xi_x, \eta_x, \xi_y, \eta_y$  = metrics;  $\hat{J}$  = Jacobian defined as  $\hat{J} \equiv x_\xi y_\eta - x_\eta y_\xi$ ;  $U$  and  $V$  = contravariant components of velocity vectors;  $M$  and  $N$  = contravariant components of discharge fluxes;  $n_*$  = Manning's roughness coefficient. Eqs.(1) and (2) denote the mass and momentum conservation laws, and Eq.(3) means the chain rule and Eq.(4) shows the definitions of the Reynolds stress terms in a simple closure model (zero-equation model) of shallow-water turbulence employed in this study, respectively.

## ADJOINT ANALYSIS OF SHALLOW-WATER EQUATIONS

### Definition of objective function

The framework of the inverse problem to identify Manning's roughness coefficient in open channel flows is presented here, and this can be carried out by minimizing the following objective function  $J$  defined as the time and space integration of the least square errors between simulated data and observation data, i.e.,

$$J = \frac{1}{2} \int_0^T \iint_D \left[ K_H \delta^H (\Delta H)^2 + K_u \delta^u (\Delta u)^2 \right] d\xi d\eta dt \quad (5a)$$

$$\Delta H = H^{cal} - H^{ob}, \quad \Delta u = u^{cal} - u^{ob} \quad (5b)$$

where  $T$  = computational period,  $D$  = spatial domain of integration,  $H^{ob}$  = observed water level,  $H^{cal}$  = simulated water level,  $u^{ob}$  = observed velocity and  $u^{cal}$  = simulated velocity,  $\Delta H$  and  $\Delta u$  = data misfit,  $\delta^H$  and  $\delta^u$  = Dirac's delta, and  $K_H$  and  $K_u$  are weighting factors, respectively. As the objective function  $J$  is the function of Manning's roughness coefficients, the minimization of  $J$  will result in the optimal estimation of the coefficients.

#### Variational approach

In order to minimize the objective function and ensure that the flow velocity and the water level satisfy the shallow-water model (1)–(4), the objective function can be reconstructed as follows:

$$J^* = J + \int_0^T \iint_D \left( \lambda_h f_h + \lambda_M f_M + \lambda_N f_N + \lambda_m f_m + \lambda_n f_n \right. \\ \left. + \lambda_{\tau_{xx}} f_{\tau_{xx}} + \lambda_{\tau_{xy}} f_{\tau_{xy}} + \lambda_{\tau_{yy}} f_{\tau_{yy}} \right) d\xi d\eta dt \quad (6)$$

where the functional  $J^*$  is referred to as the augmented objective function;  $\lambda_h, \lambda_M, \lambda_N, \lambda_m, \lambda_n, \lambda_{\tau_{xx}}, \lambda_{\tau_{xy}}$  and  $\lambda_{\tau_{yy}}$  are the Lagrange multipliers with respect to the dependent variables of  $h, M, N, m, n, \tau_{xx}, \tau_{xy}$  and  $\tau_{yy}$ . According to the variational principle, the first variation of  $J^*$  must be zero so as to minimize the objective function  $J$  in Eq.(5a) with the constraint which is expressed as the mathematical model (1)–(4). Consequently, the following equation is derived:

$$\delta J^* = \int_0^T \iint_D \left( f_h^* \delta h + f_M^* \delta M + f_N^* \delta N + f_m^* \delta m + f_n^* \delta n \right. \\ \left. + f_{\tau_{xx}}^* \delta \tau_{xx} + f_{\tau_{xy}}^* \delta \tau_{xy} + f_{\tau_{yy}}^* \delta \tau_{yy} + f_n^* \delta n \right) d\xi d\eta dt \quad (7)$$

where  $\delta h, \delta M, \delta N, \delta m, \delta n, \delta \tau_{xx}, \delta \tau_{xy}, \delta \tau_{yy}$  and  $\delta n$  are the variations of the dependent variables in the shallow-water model and  $f_h^*, f_M^*, f_N^*, f_m^*, f_n^*, f_{\tau_{xx}}^*, f_{\tau_{xy}}^*, f_{\tau_{yy}}^*$  and  $f_n^*$  are differential operators regarding the Lagrange multipliers.

According to the extremum conditions, all terms multiplied by the variations of the dependent variables in Eq.(7) can be set to zero except for the control variable, respectively, in order to establish the optimal condition. The adjoint equations are therefore derived in a continuous form as follows:

$$f_h^* = 0; f_M^* = 0; f_N^* = 0; f_m^* = 0; f_n^* = 0; f_{\tau_{xx}}^* = 0; f_{\tau_{xy}}^* = 0; f_{\tau_{yy}}^* = 0 \quad (8)$$

In addition, the gradient of the augmented objective function with respect to the unknown variable is expressed as follows:

$$\frac{\partial J^*}{\partial n_i} = \int_0^T \iint_{D_i} f_n^* d\xi d\eta dt \quad (9)$$

where  $n_i$  denotes the Manning's roughness coefficient of the specified domain  $D_i$  in the whole computational

domain.

## NUMERICAL PROCEDURE

### *Discretization of governing equations*

Eqs.(1)~(4) are discretized by the finite difference method based on the conservative concept employed in the finite volume method. Time development of depth-averaged velocity and water depth is computed by the explicit Euler scheme. The spatial derivatives are discretized by means of the second-order central scheme, except for the advection terms which are discretized by the first-order upwind scheme. The boundary conditions needed for solving Eqs.(1)~(4) are the discharge hydrograph across the channel at the upstream end and water surface elevation at the downstream end in the case of the subcritical flows. In addition, the slip condition for the depth-averaged velocity parallel to the boundary wall is adopted at both banks in a compound open-channel so that the velocity perpendicular to the wall is zero. A detailed description of the discretization procedure can be found in the paper by Nagata et al. (7).

### *Parameter identification methodology*

In order to minimize the objective function defined in Eq.(5) and to estimate the optimal parameters finally, an iterative procedure is required due to the nonlinearity nature of the problem. We applied a quasi-Newton method with a BFGS algorithm to the problem mentioned above. In this method, an inverse Hessian matrix of the objective function is evaluated approximately by means of a steepest descent direction in order to estimate the Newton direction of the function.

The steepest descent direction can be efficiently calculated by Eq.(9) in the adjoint-equation method. This is one of the advantages of the adjoint-equation method among the optimization ones which deal with the sensitivity of the control variables. The integrand of the equation (9) is a function of the adjoint variables or the Lagrange multipliers, which can be computed by the adjoint equations (8).

In spite of the usefulness of the adjoint method in the optimization problems, several previous studies have pointed out the difficulties inherent with the inverse estimation of the parameters. As noted by Yeh (8), the inverse problem is often posed badly, and the inverse analysis occasionally results in the nonphysical solution. Thus, we imposed a boundary restriction on the estimated parameters in every iteration of the optimization procedure in order to preserve the physical meaning of the Manning's roughness coefficient. In this study, the bound constraint is set as follows:

$$n_{\min} \leq n \leq n_{\max} \quad (10)$$

where the  $n_{\min}$  and  $n_{\max}$  represent lower and upper bounds on the value of Manning's roughness coefficients, which can be specified by means of some relevant engineering documents and experiences of engineers. In this study,  $n_{\min}$  and  $n_{\max}$  are set to be 0.01 and 0.09, respectively.

## APPLICATIONS AND DISCUSSIONS

### *Setting of numerical tests*

The performance of the proposed method for identifying the Manning's roughness coefficients in a hypothetical

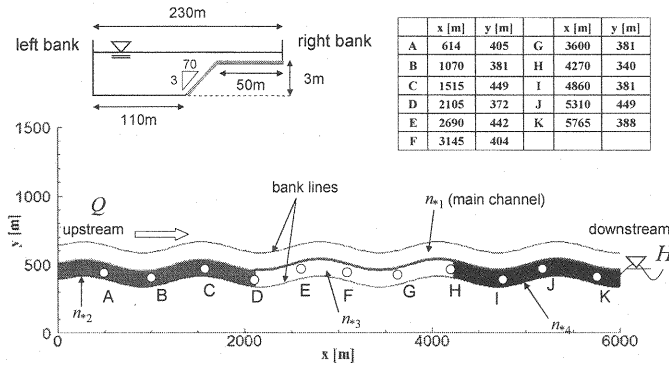


Fig.1 Schematic of meandering open-channel with a flood plain on a right-side bank

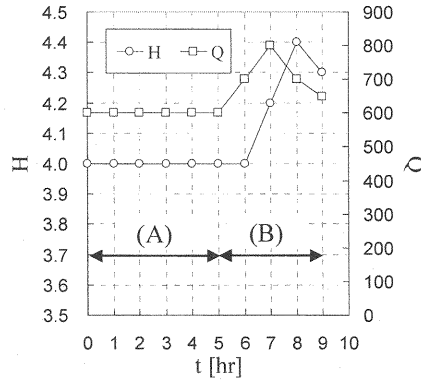


Fig.2 Time-dependent boundary conditions of discharge  $Q$  [m³/s] and water level  $H$  [m]

meandering open-channel flow was verified with several series of the identical twin experiments. In these experiments, first of all, the meandering open-channel flow is computed by using a set of specified parameters of Manning's roughness coefficients of the flood plain, and some simulated variables such as the water level and depth-averaged flow velocity at several locations are stored as the "observed" data on a regular schedule. These data are assumed to be error-free for identifying these specified parameters inversely. Secondly, we start a new simulation with a new set of parameters which is quite different from the previously specified set (or "true" set). Then, the aforementioned identification procedure will search and find optimal values of the parameters. By means of such a procedure in these experiments, we can investigate the feasibility and the reliableness of the proposed method. The reason for this is because we can compare precisely the estimated values of the parameters with the true ones.

By means of this approach, we attempted to identify the distributed parameters of a flood plain in a single meandering open-channel. Fig.1 illustrates a hypothetical channel with the flood plain on the right-side bank. The roughness coefficient of the main channel indicated as the variable  $n_1$  is fixed to be 0.03 through the whole procedure, while the longitudinally distributed coefficients  $n_2, n_3$  and  $n_4$  of the flood plains are identified by the method proposed here. The "true" values of  $n_2, n_3$  and  $n_4$  are 0.035, 0.060 and 0.055 for any cases in the tests. It is assumed that these parameters do not vary with time in this study. The marks A ~ K shown in the figure denote the locations of the observation station and the table in the figure shows the position of the stations in 2-D Cartesian coordinates. The boundary conditions are taken into account as follows: the discharge is set at the upstream end and the water level is imposed at the downstream end.

Table 1 Estimated parameters with data of water level assimilated at 10 minutes time interval

Case	Observation station					First guess	Estimates $\times 10^2$		
							$n_{s2}$	$n_{s3}$	$n_{s4}$
A-1	B	F	J			0.07	3.50	6.00	5.50
A-2	B	F	J			0.03	9.00	2.95	7.99
A-3	B	F	J			0.05	3.50	6.00	5.50
A-4	A	E	I			0.07	3.50	6.00	5.50
A-5	A	E	I			0.03	2.70	6.60	8.77
A-6	A	E	I			0.05	3.50	6.00	5.50
A-7	C	G	K			0.07	4.36	5.84	5.52
A-8	C	G	K			0.03	2.70	6.60	8.77
A-9	C	G	K			0.05	3.50	6.00	5.50
A-10	B	D	F	H	J	0.07	3.50	6.00	5.50
A-11	B	D	F	H	J	0.03	3.50	6.00	5.50
A-12	B	D	F	H	J	0.05	3.50	6.00	5.50

The numerical conditions are as follows: the two-dimensional grid numbers are 141 12, with 141 sections in the streamwise direction or  $x$ -direction and 12 grids in the cross-sectional direction or  $y$ -direction. Time increment  $\Delta t$  in the simulation is 1.5sec throughout the numerical experiments As shown in the Fig.2, the discharge  $Q$  and the water level  $H$  are kept constant during the period (A) and they vary linearly in time during the period (B). The simulation starts from a still-water condition, and the period (A) needs to be set prior to the period (B) because the flow field should be indentified uniquely with respect to a set of parameters, and the period (B) are required to assimilate the observation data into the model. The longitudinal channel slope is set at zero. In addition, the horizontal kinetic viscosity used to calculate the Reynolds stresses is determined by means of the Richardson's empirical formula.

As shown with the marks A ~ K in the Fig.1, the observation stations are placed longitudinally in the flood plains with the same interval. In this study, two kinds of experiments for verifying the method were carried out. The difference between two experiments is whether the observation data include the artificial random perturbations or not. In practice, the real data do not always fit the numerical model, due both to observational errors and to imperfections in the model itself. Therefore, it is important to examine the stability of the estimated parameters to avoid such errors.

#### Parameter estimation

Table 1 shows the identification results of the parameters (Manning's roughness coefficients) with the observation data of the water level assimilated at 10 minutes time interval. The first guess means the initial data of the parameters in the iteration procedure, and the value is the same in every parameter for each case. The iteration number is mandatorily within 50 regardless of the results. It was found in this series that the algorithm successfully converged from the starting point to the final estimate except for the case A-2, A-5, A-7 and A-8, and that the parameters are estimated well to at least three significant digits in almost cases, if the first guess is set near the average of the "true" values and the observation data are sufficiently assimilated at more observation stations, namely, the errors of the estimated parameters are generated depending on their first values in the iteration process as well as on the location of the observation stations.

Fig.3 shows the iteration history of identifying the parameters both in the case A-1 and in the case A-3. At the beginning of the iteration in the case A-1, the value of the parameter  $n_{s3}$  reached near the upper bound. Then, the estimated value gradually approached to the "true" values step by step in the following iterations. Finally, each parameter converged to the "true" value in each case. After twelve iterations, the relative error of each parameter was

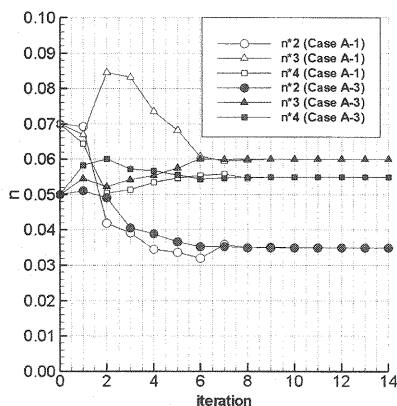


Fig.3 Iteration history of identifying parameters (Case A-1 and Case A-3)

Table 2 Estimated parameters with data of water level assimilated at 60 minutes time interval

Case	Observation station					First guess	Estimates $\times 10^2$		
							$n_{k2}$	$n_{k3}$	$n_{k4}$
B-1	B	F	J			0.07	4.61	5.16	5.69
B-2	B	F	J			0.05	3.43	6.08	5.49
B-3	A	E	I			0.07	3.50	6.00	5.50
B-4	A	E	I			0.05	3.50	6.00	5.50
B-5	C	G	K			0.05	3.50	6.00	5.50
B-6	B	D	F	H	J	0.05	3.50	6.00	5.50
B-7	B	D	F	H	J	0.07	3.50	6.00	5.50
B-8	B	D	F	H	J	0.03	3.50	6.00	5.50

found to be estimated less than  $10^{-5}$  in each case. The parameter can be therefore identified with a high accuracy. Moreover, it was found in successful cases that the parameters were precisely identified without the boundary restriction represented in Eq.(10).

Table 2 shows the identified parameters with use of the observation data of the water level assimilated at 60 minutes time interval. The time interval in the series B is longer than that in the series A, and consequently the amount of the observation data decreased relatively in comparison with the series A. Therefore, the experimental conditions of the failed cases in the series A were not taken into account in the series B. We found that the identification was successful if the data was sufficiently assimilated at the five observation stations, and that the identification failed in two cases (B-1 and B-2) with the data recorded in middle region in each flood plain; nevertheless, the estimated values of the parameters were not so different from the true ones in the case B-2.

Table 3 shows the identified parameters by means of the observation data of the depth-averaged streamwise flow velocity assimilated at 60 minutes time interval. In this series, the estimations in almost all the cases were successfully completed except for the case C-8, in which the observation data were obtained at the downstream region in each flood plain. From this result and Table 2, it can be seen that the observation data recorded at more upstream stations is effectively used to identify the roughness coefficients in the shallow-water adjoint model.

#### *Sensitivity of parameter estimation*

In the above numerical experiments, the synthetic observation data were calculated by the shallow-water model



Table 3 Estimated parameters with data of depth-averaged streamwise flow velocity assimilated at 60 minutes time interval

Case	Observation station					First guess	Estimates $\times 10^2$		
							$n_2$	$n_3$	$n_4$
C-1	B	F	J			0.07	3.50	6.00	5.50
C-2	B	F	J			0.03	3.50	6.00	5.50
C-3	B	F	J			0.05	3.50	6.00	5.50
C-4	A	E	I			0.07	3.50	6.00	5.50
C-5	A	E	I			0.03	3.50	6.00	5.50
C-6	A	E	I			0.05	3.50	6.00	5.50
C-7	C	G	K			0.07	3.50	6.00	5.50
C-8	C	G	K			0.03	4.84	9.00	8.56
C-9	C	G	K			0.05	3.50	6.00	5.50

Table 4 Estimated parameters with data of water level combined with random noise generated by a normal random number, assimilated at 10 minutes time interval (standard deviation: 0.01m)

Case	Observation station					First guess	Estimates $\times 10^2$		
							$n_2$	$n_3$	$n_4$
D-1	B	F	J			0.05	3.74	5.76	5.49
D-2	A	E	I			0.05	3.58	5.80	5.51
D-3	C	G	K			0.05	2.13	6.53	5.37
D-4	B	D	F	H	J	0.07	3.52	5.99	5.38
D-5	B	D	F	H	J	0.03	3.52	5.99	5.38
D-6	B	D	F	H	J	0.05	3.52	5.99	5.38

itself. As long as sufficient data are assimilated in the adjoint model, the exact parameter values can be identified with a high accuracy, as presented in the above results. Here, we examined the sensitivity of parameter estimation, by putting artificial random disturbances into the observation data. In these tests, random noise was generated by a normal random number with a standard deviation which is roughly determined on the basis of the accuracy of observation equipments frequently installed in practical works.

Table 4 shows the identified parameters with use of the observation data of the water level assimilated at 10 minutes time interval. In this series, the standard deviation is set to be 0.01m. Each result shown in the table is the average of a subset of numerical experiments assimilated by the several observation data which include the random disturbances generated with the same standard deviation. The test conditions such as the observation locations and first guesses were arranged by considering the results in the series A. We found that the estimates were almost similar to the "true" values in the cases with the five stations, and that the estimates in the cases with the three stations were not so much different from the true values except for the case D-3. That means the optimum result can be obtained if the assimilated data are collected in more upstream stations. Similar results are recognized in Table 3.

Table 5 shows the identified parameters with use of the observation data of the depth-averaged streamwise flow velocity assimilated at 10 minutes time interval. In this series, the standard deviation is 0.1m/s. As explained in the results of the series D, each result shown in the table is the average of a subset of numerical experiments. The estimates are almost the same and little difference among the cases is found in this series. More observational data contribute slightly to an improvement of the parameter identification; however, the effect is limited in comparison with the cases assimilated by the data of the water level. This is partly because the result might depend on the magnitude of the standard deviation of the random noise added into the assimilated data.

Table 5 Estimated parameters with data of depth-averaged streamwise flow velocity combined with random noise generated by a normal random number, assimilated at 10 minutes interval (standard deviation: 0.1m/s)

Case	Observation station)					First guess	Estimates $\times 10^2$		
							$n_{s2}$	$n_{s3}$	$n_{s4}$
E-1	B	F	J			0.07	3.73	5.77	5.69
E-2	B	F	J			0.03	3.73	5.77	5.68
E-3	B	F	J			0.05	3.73	5.77	5.69
E-4	A	E	I			0.07	3.73	5.78	5.72
E-5	A	E	I			0.03	3.72	5.79	5.73
E-6	A	E	I			0.05	3.72	5.79	5.73
E-7	C	G	K			0.07	3.70	5.76	5.72
E-8	C	G	K			0.03	3.70	5.76	5.72
E-9	C	G	K			0.05	3.70	5.76	5.72
E-10	B	D	F	H	J	0.07	3.72	5.99	5.88
E-11	B	D	F	H	J	0.03	3.72	5.98	5.88
E-12	B	D	F	H	J	0.05	3.72	5.98	5.88

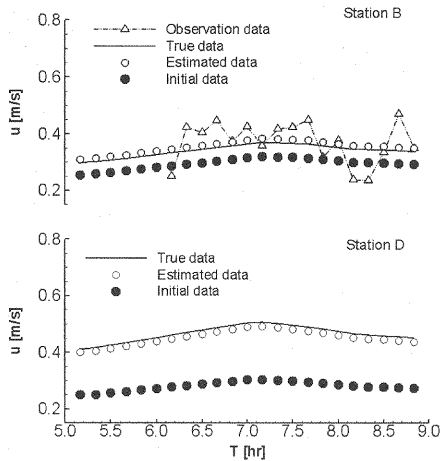


Fig.4 Time series of depth-averaged flow velocity at the station B as well as at the station D (case E-1)

Fig.4 shows the time series of the depth-averaged streamwise flow velocity recorded at the station B as well as at the station D in the case of E-1. In this figure, a set of filled circles denotes time-series of the velocity data during the assimilated period (see the period (B) shown in Fig.2). These data are calculated by means of the forward model with a set of parameters which are not optimized. A set of open circles represents time-series of the velocity data calculated with the optimized parameters during the period. In addition, a set of open triangles denotes the time-series of the observed data used for the assimilation process. The observed data was not available at the station D in this case. The line which is added in the figure shows the time series of the velocity at the station B, which is calculated with the true values of the parameters. We found that the velocity profile can be suitably retrieved at the station B by means of the data assimilation. Moreover, the profile at the station D approaches to the “true” profile. The result indicates that the whole flow field in the shallow-water model can be estimated well with the given boundary data, once we can identify appropriately the distributed Manning’s roughness coefficients by means of the data assimilation.

## CONCLUDING REMARKS

The inverse methodology to identify the bed roughness coefficients of open-channels with flood plains was proposed in this study, and was verified by the identical twin experiments. In order to minimize the objective function, which can be evaluated based on the discrepancy between the simulated data and observation data, the Lagrange multiplier method was used for the coefficient identification. The adjoint model was developed by both the multiplier method and the shallow-water model. The gradient of the function with respect to the control variables (or the coefficients) was efficiently calculated by the adjoint model, and the optimal values of the coefficients were determined by the quasi-Newton method.

The results of several numerical tests by means of the identical twin experiments showed that the coefficients can be accurately identified and these estimates are stably obtained with respect to random noise in the data, provided that sufficient data are available at observation stations. Therefore, we conclude that the proposed method is promising, if it is applied to the practical works of identifying the roughness coefficients in the shallow-water flows. This method is valid especially in situations where much data such as river discharge and the water levels are fully observed in the upstream and downstream boundaries with a high degree of accuracy.

## REFERENCES

1. Atanov, G.A., Evseeva, E.G. and Meselhe, E.A.: Estimation of roughness profile in trapezoidal open channels, *J. Hydr. Eng.*, ASCE, Vol.125, No.3, pp.309-312, 1999.
2. Sanders, B.F. and Katopodes, N.D.: Control of canal flow by adjoint sensitivity method, *J. Irrigation and Drainage Eng.*, ASCE, Vol.125, No.5, pp.287-297, 1999.
3. Ramesh, R., Datta, B.B.S.M. and Narayana, A.: Optimal estimation of roughness in open-channel flow, *J. Hydr. Eng.*, ASCE, Vol.126, No.4, pp.299-303, 2000.
4. Dulhoste, J.-F., George, D. and Besancon, G.: Nonlinear control of open-channel water flow based on collocation control model, *J. Hydr. Eng.*, ASCE, Vol.130, No.3, pp.254-266, 2004.
5. Sulzer, S., Rutschmann, P. and Kinzelbach, W.: Flood discharge prediction using two-dimensional inverse modeling, *J. Hydr. Eng.*, ASCE, Vol.128, No.1, pp.46-54, 2004.
6. Ding, Y. and Wang, S.S.Y.: Identification of Manning's roughness coefficients in channel network using adjoint analysis, *Int. J. Comput. Fluid Dynam.*, Vol.19, No.1, pp.3-13, 2005.
7. Nagata, N., Hosoda, T. and Muramoto, Y.: Numerical analysis of river channel processes with bank erosion, *J. Hydr. Eng.*, Vol.126, No.4, pp.243-252, 2000.
8. Yeh, W.W.-G.: Review of parameter identification procedures in ground water hydrology: the inverse problem, *Water Resour. Res.*, Vol.22, No.2, pp.95-108, 1986.

## APPENDIX – NOTATION

The following symbols are used in this paper:

$D$  = spatial domain of integration or computational domain;

$f_h$	= differential operators of mass balance;
$f_M, f_N$	= differential operators of momentum conservations;
$f_m, f_n$	= differential operators of the definitions of relevant variables $m, n$ ;
$f_{\tau_{xx}}, f_{\tau_{xy}}, f_{\tau_{yy}}$	= differential operators of the definitions of relevant variables $\tau_{xx}, \tau_{xy}, \tau_{yy}$ ;
$f_\theta^*$	= differential operators of regarding the Lagrange multipliers with respect to $\theta$ ;
$g$	= gravity acceleration;
$h$	= local water depth;
$H$	= water level;
$J$	= objective function or cost function;
$J^*$	= augmented objective function;
$\hat{J}$	= Jacobian defined as $\hat{J} = x_\xi y_\eta - x_\eta y_\xi$ ;
$k$	= depth-averaged turbulent kinematic energy;
$K_H, K_u$	= weighting factors on relevant variables;
$M, N$	= $x$ - and $y$ - components of discharge flux;
$n_*$	= Manning's roughness coefficient;
$Q$	= discharge;
$t$	= time;
$T$	= computational time;
$u, v$	= $x$ - and $y$ - components of velocity vectors;
$m, n$	= $x$ - and $y$ - components of discharge fluxes;
$M, N$	= contravariant components of discharge fluxes;
$U, V$	= contravariant components of velocity vectors;
$x, y$	= 2-D Cartesian coordinates;
$\Delta$	= data misfit, for example, $\Delta H$ = data misfit of water level;
$\delta_\theta$	= variation with respect to the variable $\theta$ ;
$\delta^H, \delta^u$	= Dirac's delta on relevant variables;
$\varepsilon$	= horizontal eddy viscosity;

$\lambda_\theta$	= Lagrange multiplier with respect to the variable $\theta$ ;
$\xi, \eta$	= 2-D boundary fitted coordinates;
$\xi_x, \eta_x, \xi_y, \eta_y$	= metrics, for instance, $\xi_x = \partial \xi / \partial x$ ;
$\sigma$	= local curvature along the channel coordinate ( $s$ axis);
$\tau_{xx}, \tau_{xy}, \tau_{yy}$	= Cartesian components of depth-averaged Reynolds stress tensors;
superscript <i>cal</i>	= calculated values;
superscript <i>ob</i>	= observed values
suffix <i>i</i>	= specified number, for example, $D_i$ = specified domain;
suffix <i>max</i>	= the maximum values; and
suffix <i>min</i>	= the minimum values.

(Received Jun, 30, 2010 ; revised Nov, 17, 2010)